Electronic Supplementary Material (ESI) for Journal of Materials Chemistry A.
This journal is © The Royal Society of Chemistry 2023

Supporting Information

Controllable fabrication of $Cs_2AgBiBr_6$ nanocrystal/ mesoporous black TiO_2 hollow spheres composite for photocatalytic benzyl alcohol oxidation

Menghan Yu[1], Nan Wang[1], Kuo Lin[1], Dongxue Song[1], Jie Chen[1], Teng Liang[2], Jianhui Sun[2], Kai Pan[1, *] and Honggang Fu[1, *]

[1] Key Laboratory of Functional Inorganic Material Chemistry, Ministry of Education, Heilongjiang University, Harbin, 150080, China

Corresponding author: kaipan@hlju.edu.cn; fuhg@hlju.edu.cn; fuhg@vip.sina.com

[2] College of Physics Science and Technology, Heilongjiang University, Harbin, 150080, China

Experimental section

Synthesis of mesoporous black TiO_2 hollow spheres

Typically, TBOT (0.1 g) and anhydrous oxalic acid (7.25 g) were dissolved into N, N-dimethylformamide (65 mL) and stirred for 45 minutes. Then, the mixture was transformed into a 100 mL autoclave and maintained at 170 °C for 12 hours. the resulting product was washed by ethanol and water for several times. The sample was dried at 60 °C. Subsequently, the product was refluxed with ethylenediamine aqueous solution (pH=10). The obtained powders were washed with deionized water several times and dried at 60 °C overnight. Finally, the resulting samples were calcined in air at 500 °C and in hydrogen at 600 °C to form mesoporous black TiO_2 hollow spheres.

Preparation of lead-free $Cs_2AgBiBr_6$ nanocrystals

The monodisperse $Cs_2AgBiBr_6$ nanocrystals was prepared with a standard Schlenk line. First, bismuth acetate (0.097 g), silver acetate (0.042 g), cesium acetate (0.136 g) were put into a three-necked flask with 5 ml octadecene, 1.25 ml oleylamine, 0.25ml oleic acid as mixed solvents for dissolution. Then, the solution was heated into 120°C for 60 min. Third, it was heated to 145°C, and 2.5ml trimethylbromosilane was quickly injected into solution. When the solution changed from brown into yellow, monodisperse $Cs_2AgBiBr_6$ nanocrystals was obtained. The sample was washed and re-

dispersed with n-hexane for several times.

Characterization

The crystal structure was analyzed by Bruker D8 Advance X-ray powder diffraction (Cu Kα, λ = 1.5406 Å, 40 kV, 40 mA) with a scanning speed of 10° /min and a step size of 0.01° to obtain XRD patterns. Scanning electron microscope (SEM, acceleration voltage 5 kV, Hitachi S-4800) and transmission electron microscope (TEM, JEOL JEM-2100) were used to investigate the surface morphology of the samples. X-ray photoelectron spectroscopy (XPS, Kratos, ULTRA AXIS DLD) using monochromatic Al Kα (hv= 1486.6 eV) radiation. All binding energies were calibrated with reference to the C 1s peak at 284.6 eV. The UV-visible diffuse reflectance spectra (UV-vis DRS) of the samples were obtained from the UV-vis spectrophotometer test (Shimadzu UV-2550). The function works of black TiO_2, $Cs_2AgBiBr_6$ and $Cs_2AgBiBr_6$/black TiO_2 were determined using the Scanning Kelvin probe (SKP5050 system Scotland) at the room temperature condition. Electron paramagnetic resonance (EPR) measurements were performed on a Brucker EMX plus type spectrometer at the room temperature. N-tert-Butyl-α-phenylnitrone (PBN) was used as a trapping reagent to characterize the suspension of benzyl alcohol after illumination. Surface photovoltage spectroscopy (SPS) using a home-built device with a lock-in amplifier (SR830) synchronized with an optical chopper (SR540). Transient-state surface photovoltage spectroscopy (TPV) was tested at room temperature by using a second harmonic Nd: YAG laser (Lab-130-10H, Newport, Co.) excited by a radiation pulse with 10 ns width. The signal was amplified with a preamplifier and then registered by a 1 GHz digital phosphor oscilloscope (DPO4104B, Tektronix).

Photocatalytic activity

We have investigated the photocatalytic activity of $Cs_2AgBiBr_6$ nanocrystal/black TiO_2 was carried out in a photocatalytic reaction cell. 10 mg of photocatalyst was dispersed in 5 ml of cyclohexane and 0.1mmol of benzyl alcohol solution. Prior to irradiation, the entire photocatalytic reactor was evacuated and filled with N_2 to ensure that the interior is free of air and in an anaerobic state followed by a 300 W Xenon lamp visible light irradiation equipped with simulated sunlight (AM1.5G) for 8 h at normal temperature and pressure. After the reaction done, H_2 amount was tested by a gas chromatography (GC), and the liquids were detected by gas chromatography-mass spectrometry (GC-MS). The conversion and selectivity of photocatalytic oxidation of benzyl alcohol can be calculated by the following equation (S1) and (S2):

Conversion（%）：$X=（C_0-C_1/C_0\times 100)$ (S1)

Selectivity（%）：$S=100\times C_P/（C_0-C_1）$ (S2)

where C_0 and C_1 and C_P are the concentration of benzyl alcohol before and after the reaction, and the amount of target product benzaldehyde, respectively.

Photoelectrochemical measurements

All electrochemical and photoelectrochemical measurements were performed by a standard three-electrode system (Princeton Versa STAT). In general, Ag/AgCl was used as the reference electrode and platinum as the counter electrode, and the prepared FTO membrane electrode was used as the working electrode. A solution of 1-butyl-3-methylimidazolium hexafluorophosphate in dichloromethane was used as an electrolyte (0.1 M) and purged with N_2 for 3 h before the test. Mott-Schottky tests were performed at three different frequencies (800, 1000, 1200 Hz) to obtain the spectra. Transient photocurrent responses were also collected under illumination with a bright and dark AM 1.5G light source, as well as electrochemical impedance spectra under illumination conditions.

Active species trapping experiments

Small amounts of methanol (CH_3OH), benzoquinone ($C_6H_4O_2$) and carbon tetrachloride (CCl_4) were added to the photocatalytic reaction system to find out the effect of the corresponding active substances in the photocatalytic reaction, respectively. Among them, methanol was the h^+ scavenger, benzoquinone was the $\cdot O^{2-}$ radical scavenger, and carbon tetrachloride was the e^- scavenger.

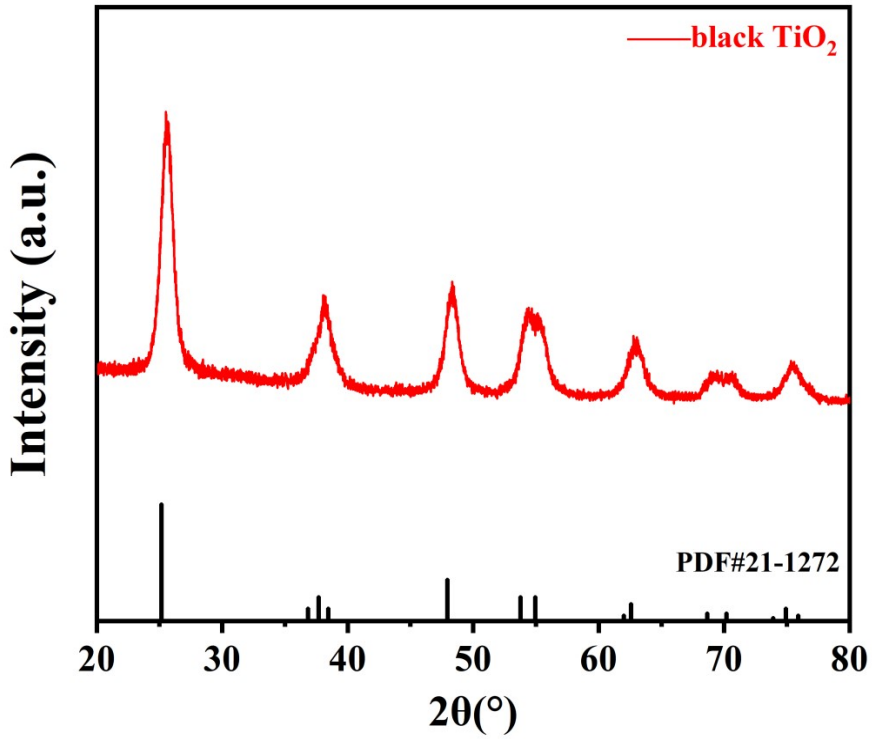

Fig. S1. XRD pattern of black TiO_2 hollow spheres.

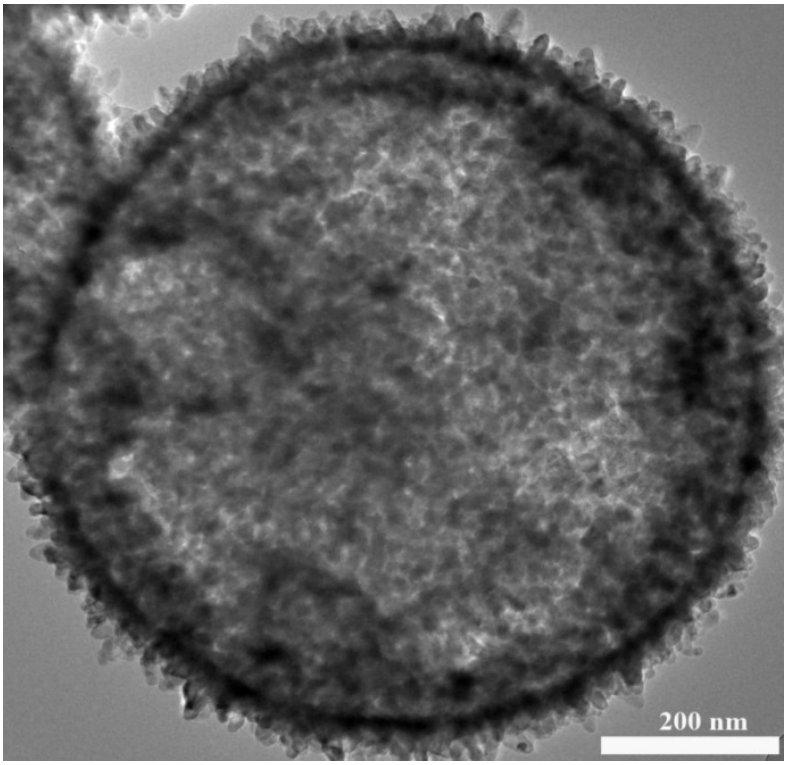

Fig. S2. TEM image of black TiO_2 hollow spheres.

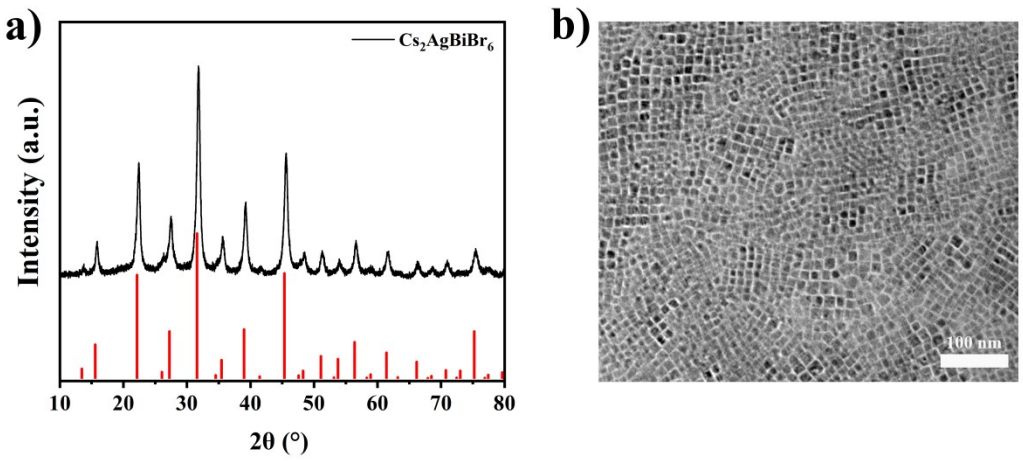

Fig. S3. XRD (a) and TEM images (b) of $Cs_2AgBiBr_6$ nanocrystals.

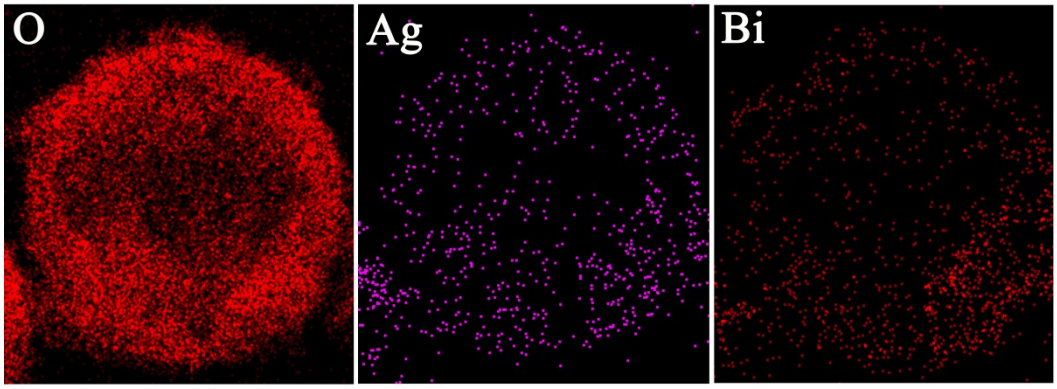

Fig. S4. Element mapping images of O, Ag, and Bi.

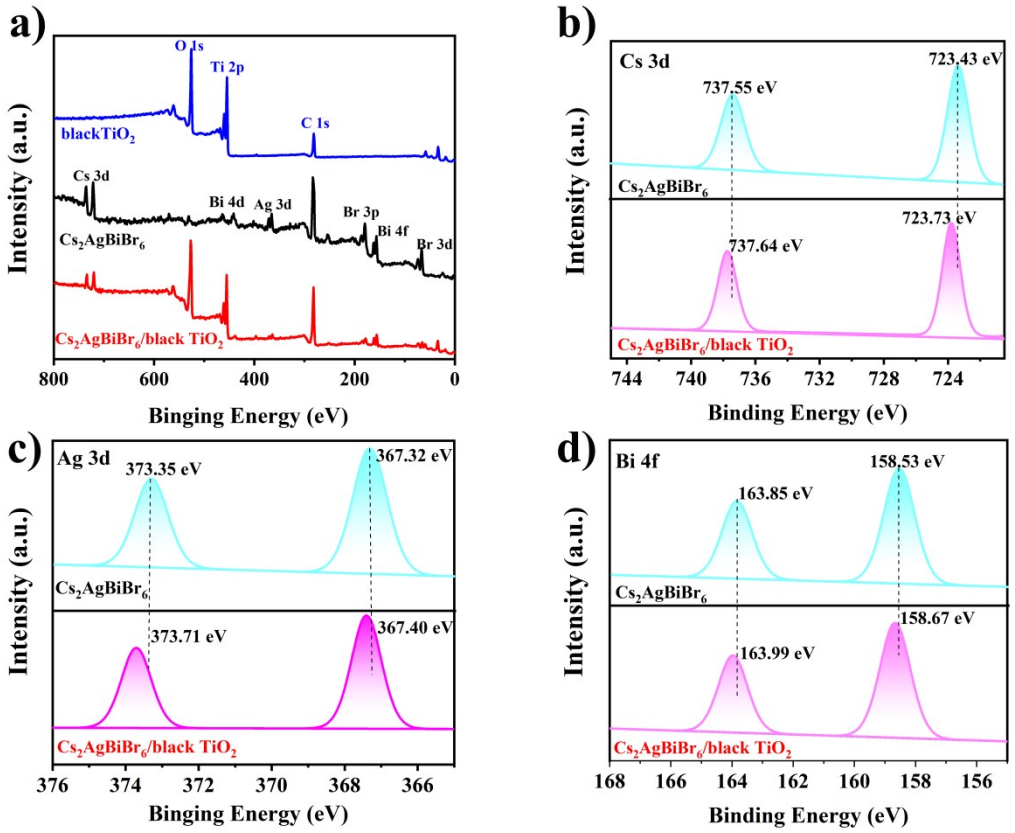

Fig. S5. (a) Survey XPS spectra of the black TiO_2, $Cs_2AgBiBr_6$ nanocrystals and $Cs_2AgBiBr_6$ nanocrystal/black TiO_2. (b-d) XPS spectra of Cs 3d, Ag 3d, and Bi 4f of samples.

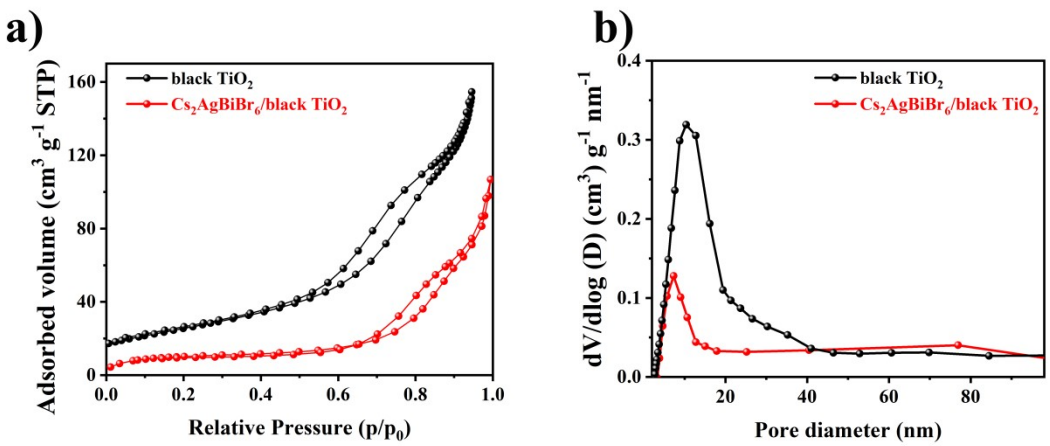

Fig. S6. (a) nitrogen sorption isotherms, and (b) corresponding pore size distribution curves of $Cs_2AgBiBr_6$/black TiO_2 tandem heterojunctions, and black TiO_2 microspheres, respectively.

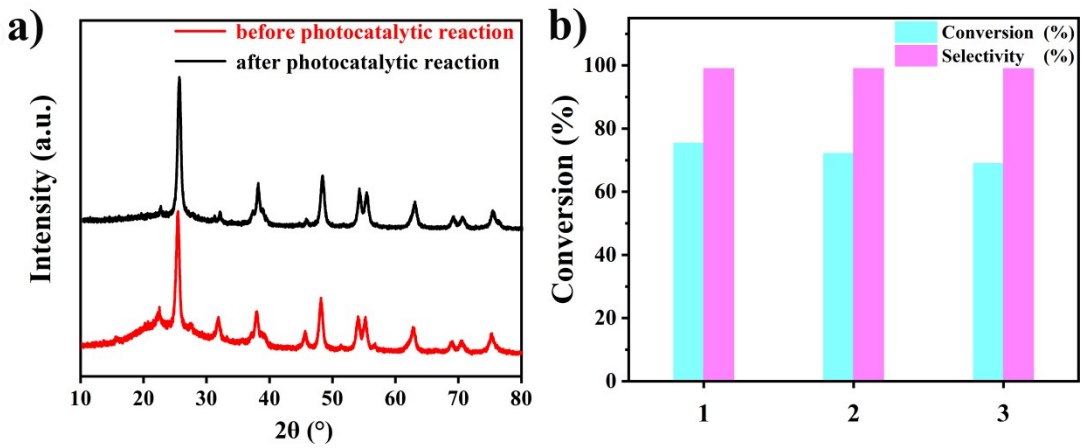

Fig. S7. Benzyl alcohol selective oxidation stability of $Cs_2AgBiBr_6$ nanocrystal /black TiO_2.

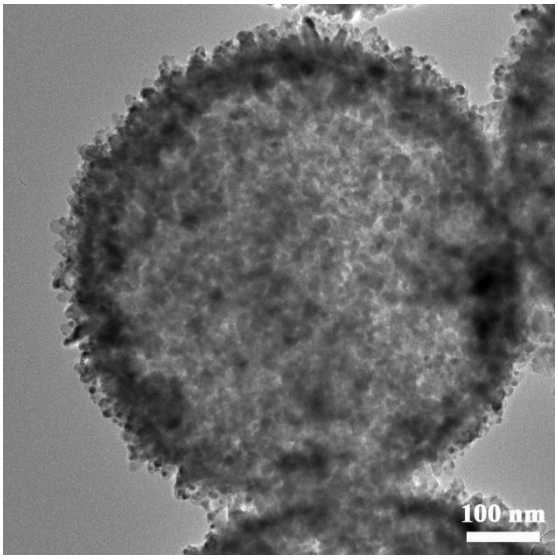

Fig. S8. TEM image of $Cs_2AgBiBr_6$ nanocrystal/black TiO_2 after three times reactions.

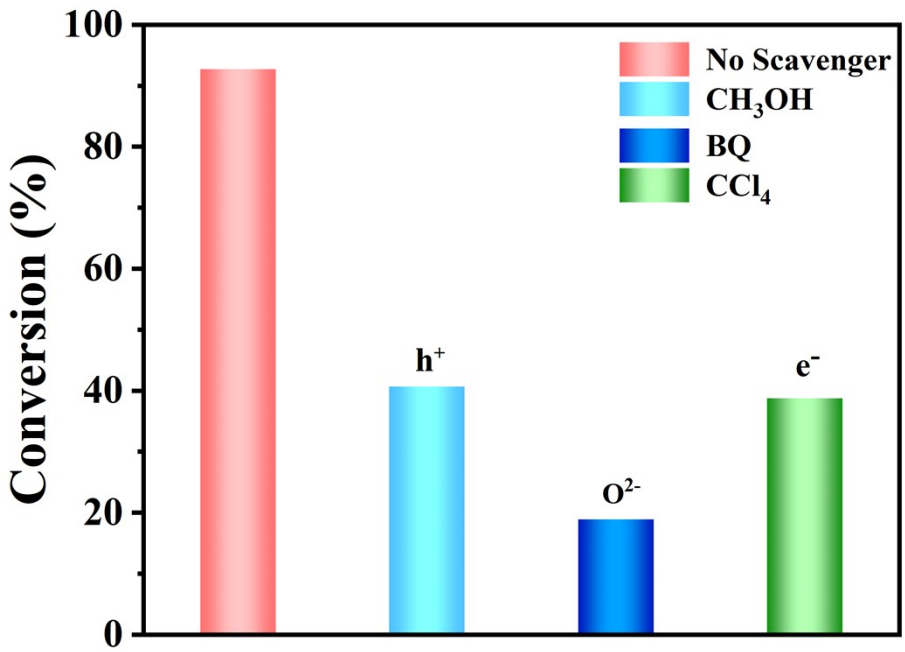

Fig. S9. Photocatalytic activity of $Cs_2AgBiBr_6$ nanocrystal/black TiO_2 for selective oxidation of benzyl alcohol with or without different scavengers at O_2 atmosphere.

Table S1. Summary of the photocatalytic selective oxidation of benzyl alcohol of TiO_2-based catalysts.

Photocatalyst	Reaction conditions	Atmosphere	Conversion	Selectivity	Ref.
5-$Cs_2AgBiBr_6$/black TiO_2	300W Xe lamp AM 1.5G, 8h	N_2	75.39%	99%	This Work
5-$Cs_2AgBiBr_6$/black TiO_2	300W Xe lamp AM 1.5G, 8h	O_2	92.72%	85.24%	This Work
5-$Cs_2AgBiBr_6$/black TiO_2	300W Xe lamp λ＞400nm, 8h	N_2	18.2%	99%	This Work
5-$Cs_2AgBiBr_6$/black TiO_2	300W Xe lamp λ＞400nm, 8h	Air	27.56%	99%	This Work
15% $FAPbBr_3$/TiO_2	300W Xe lamp λ＞420nm, 8h	O_2	63%	99%	S1
Bi_2MoO_6@TiO_2NTA	300W Xe lamp AM 1.5G, 8h	O_2	67.4%	98.6%	S2
TiO_2/WO_3	5W LED lamp 395＜λ＜550 nm	O_2	68%	99%	S3
I-TiO_2/ (20 wt%) CNNSs	10W blue LED lamp, 8h	O_2	29%	99%	S4
TiO_2/MAGSNC	125W lamp λ= 365 nm，4h	O_2	50%	90%	S5
QH-COF@TiO_2	300W Xe lamp λ≥420nm, 4h	O_2	77%	95%	S6
TiO_2@Ag@ZnO	300W Xe lamp AM 1.5G,1h	Air	86.2%	51.1%	S7
Pd-Zn/TiO_2	300W Xe lamp AM 1.5G, 1h, 120°C	O_2	55%	81%	S8
TBCN@3%rGO	250W Xe lamp λ＞420nm,5h	O_2	79.7%	97.3%	S9
12.4% $Cs_3Bi_2Br_9$/TiO_2	300W Xe lamp λ＞420nm, 8h	O_2	73%	97.7%	S10
$Cs_3Sb_2Br_9$-50	500W Xe lamp λ＞420nm	O_2	88%	88%	S11

$FAPbBr_3/WO_3$	300W Xe lamp AM 1.5G, 4h	O_2	65.71%	90%	S12
$CsPbX_3/W_{18}O_{49}$	150cW Xe lamp AM 1.5G,8h	O_2	72%	99%	S13
Pt-g-C_3N_4	300W Xe lamp λ＞400nm, 20h	Ar	40%	90%	S14
SA-Fe/$N_{4.5}$-C	300W Xe lamp AM 1.5G, 24h	O_2	92.7%	96.4%	S15
Bi_2MoO_6	300W Xe lamp λ＞400nm, 4h	O_2	37.4%	99%	S16
VC/CdS-15	300W Xe lamp λ＞420nm, 2h	N_2	41%	99%	S17
ZnO/C_3N_4-600	10W blue LED lamp,λ=400-405nm, 12h	O_2	74.6%	99%	S18
$ZnFe_2O_4$/UiO-66-NH_2	300W Xe lamp AM 1.5G, 5h	O_2	68%	99%	S19
AgBr@Ag@TiO_2	300 W Xe lamp λ ⩾420 nm 6h	O_2	73%	98%	S20
TiO_2@COF-3	Visible light λ> 420 nm, 30h	O_2	92.5%	99%	S21

References

S1. H. Huang, H. Yuan, K. P. F. Janssen, G. Solís-Fernández, Y. Wang, C. Y. X. Tan, D. Jonckheere, E. Debroye, J. Long, J. Hendrix, J. Hofkens, J. A. Steele and B. J. Roeffaers, *ACS Energy Lett*., 2018, **3**, 755-759.

S2. Z. Zhou, Y. N. Xie, W. Zhu, H. Zhao, N. Yang and G. Zhao, *Appl. Catal. B*, 2021, **286**, 119868.

S3. E. Safaei, S. Mohebbi and M. Irani, *J. Sol-Gel. Sci. Techn*., 2018, **87**, 170-182.

S4. B. Akhtar, H. Ghafuri and A. Rashidizadeh, *Mol. Catal*., 2021, **506**, 111527.

S5. J. C. Colmenares, W. Ouyang, M. Ojeda, E. Kuna, O. Chernyayeva, D. Lisovytskiy, S. De, R. Luque and A. M. Balu, *Appl. Catal. B*, 2016, **183**, 107-112.

S6. H. Li, H. Liu, C. Li, J. Liu, J. Liu and Q. Yang, *J. Mater. Chem. A*, 2020, **8**, 18745-18754.

S7. S. Li, J. Cai, X. Wu and F. Zheng, *Appl. Surf. Sci.,* 2018*,* **443**, 603-612.

S8. E. Nowicka, S. Althahban, T. D. Leah, G. Shaw, D. Morgan, C. J. Kiely, A. Roldan and G. J. Hutchings, *Sci.Tech. Adv. Mat.*, 2019, **20**, 367-378.

S9. A. Behera, A. K. Kar and R. Srivastava, *Inorg Chem.*, 2022,**61**,12781-12796.

S10. Q. Sun, W. Ye, J. Wei, L. Li, J. Wang, J. H. He and J. M. Lu, *J Alloy Compd.*, *2018,***893**, 162326.

S11. D. Wu, W. Sang, B. Huo, J. Wang, X. Wang, C. Chen, Q. Huang and X. Tang, *J. Catal*., 2022, **408**, 36-42.

S12. W. Wang, H. Huang, X. Ke, X. Liu, S. Yang, K. Wang, L. Huang, C. Tu, Z. Zheng, D. Luo and M. Zhang, *Mater. Design*., 2022, **215**,110502.

S13. R. Cheng, J. A. Steele, M. B. J. Roeffaers, J. Hofkens and E. Debroye, *ACS Appl. Energy. Mater.*, 2021, **4**, 3460-3468.

S14. F. Li, Y. Wang, J. Du, Y. Zhu, C. Xu and L. Sun, *Appl. Catal. B*, 2018, **225**, 258-263.

S15. Q. Wei, J. Wang and W. Shen, *Appl Catal. B*, 2021, **292**, 120195.

S16. K. Jing, W. Ma, Y. Ren, J. Xiong, B. Guo, Y. Song, S. Liang and L. Wu, *Appl Catal. B*, 2019, **243**, 10-18.

S17. M. Tayyab, Y. Liu, S. Min, R. Muhammad Irfan, Q. Zhu, L. Zhou, J. Lei and J. Zhang, *Chinese J. Catal.*, 2022, **43**, 1165-1175.

S18. X. Jiang, W. Wang, H. Wang, Z. H. He, Y. Yang, K. Wang, Z. T. Liu and B. Han, *Green Chem*., 2022, **24**, 7652-7660.

S19. J. Liu, X. Sun, B. Jiang, M. Liu, Q. Li, X. Xiao, H. Wang, M. Zheng, S. Guo, J. Wu, Y. Zhang, K. Shi and W. Zhou, *ACS Appl. Nano. Mater*., 2022, **5**, 2231-2240.

S20. P. Zhang, P. Wu, S. Bao, Z. Wang, B. Tian and J. Zhang, *Chem. Eng. J*., 2016, **306**, 1151-1161.

S21. G. Lu, X. Huang, Z. Wu, Y. Li, L. Xing, H. Gao, W. Dong and G. Wang, *Appl*. *Surf. Sci*., 2019, **493**, 551-560.